JOURNAL OF THE ROYAL SOCIETY Interface

rsif.royalsocietypublishing.org

Research

Cite this article: Caro CG, Seneviratne A, Heraty KB, Monaco C, Burke MG, Krams R, Chang CC, Coppola G, Gilson P. 2013 Intimal hyperplasia following implantation of helical-centreline and straight-centreline stents in common carotid arteries in healthy pigs: influence of intraluminal flow. J R Soc Interface 10: 20130578.
http://dx.doi.org/10.1098/rsif.2013.0578

Received: 1 July 2013
Accepted: 26 September 2013

Subject Areas:
bioengineering, biomechanics

Keywords:
helical-centreline arterial stent, swirling intraluminal blood flow, intimal hyperplasia, vessel wall hypoxia, wall shear stress, blood–wall oxygen transport

Author for correspondence:
Colin Gerald Caro
e-mail: c.caro@imperial.ac.uk

†The animal studies were carried out at: Saint Joseph's Translational Research Institute, 387 Technology Circle NW, Suite 175, Atlanta, GA 30313, USA.
‡Present address: Yale School of Medicine, Child Study Center, 230 South Frontage Road, New Haven, CT 06519, USA.

Electronic supplementary material is available at http://dx.doi.org/10.1098/rsif.2013.0578 or via http://rsif.royalsocietypublishing.org.

Royal Society Publishing
Informing the science of the future

Intimal hyperplasia following implantation of helical-centreline and straight-centreline stents in common carotid arteries in healthy pigs: influence of intraluminal flow†

Colin Gerald Caro[1], Anusha Seneviratne[1], Kevin B. Heraty[3], Claudia Monaco[2], Martin G. Burke[3], Rob Krams[1], Carlos C. Chang[4], Gianfilippo Coppola[1,‡] and Paul Gilson[3]

[1]Department of Bioengineering, Imperial College London, South Kensington Campus, Royal School of Mines Building, London SW7 2AZ, UK
[2]Kennedy Institute of Rheumatology, Roosevelt Drive, Headington, Oxford OX3 7FY, UK
[3]Veryan Medical Limited, Unit 15 City Business Centre, Brighton Road, Horsham RH13 5BB, UK
[4]Saint Joseph's Translational Research Institute, 387 Technology Circle NW, Suite 175, Atlanta, GA 30313, USA

Intimal hyperplasia (IH) is a leading cause of obstruction of vascular interventions, including arterial stents, bypass grafts and arteriovenous grafts and fistulae. Proposals to account for arterial stent-associated IH include wall damage, low wall shear stress (WSS), disturbed flow and, although not widely recognized, wall hypoxia. The common non-planarity of arterial geometry and flow, led us to develop a bare-metal, nitinol, self-expanding stent with three-dimensional helical-centreline geometry. This was deployed in one common carotid artery of healthy pigs, with a straight-centreline, but otherwise identical (conventional) stent deployed contralaterally. Both stent types deformed the arteries, but the helical-centreline device additionally deformed them helically and caused swirling of intraluminal flow. At sacrifice, one month post stent deployment, histology revealed significantly less IH in the helical-centreline than straight-centreline stented vessels. Medial cross-sectional area was not significantly different in helical-centreline than straight-centreline stented vessels. By contrast, luminal cross-sectional area was significantly larger in helical-centreline than straight-centreline stented vessels. Mechanisms considered to account for those results include enhanced intraluminal WSS and enhanced intraluminal blood–vessel wall mass transport, including of oxygen, in the helical-centreline stented vessels. Consistent with the latter proposal, adventitial microvessel density was lower in the helical-centreline stented than straight-centreline stented vessels.

1. Introduction

Intimal hyperplasia (IH) is a leading cause of obstruction and failure of vascular interventions, including arterial stents [1,2], arterial bypass grafts [3], arteriovenous grafts [4], vascular access approaches [5–8] and balloon angioplasties [9]. Suggested mechanisms for arterial stent-associated IH include low wall shear stress (WSS) [10], disturbed flow [11], stent-inflicted wall damage [12–14] and (although seemingly not widely recognized) wall hypoxia, presumed to result from stent-induced deformation of the walls of vessels and their adventitial microvessels (Ad-MV) [1,2].

The characteristics of IH may differ in the different situations, but the process is generally regarded as comprising vessel wall thickening and luminal narrowing, caused by the proliferation and accumulation of cells, including smooth muscle cells (SMCs) and extracellular matrix, in the intima [15]. Measures adopted to prevent IH development have included the administration of heparin,

Figure 1. Example of a stent with three-dimensional helical-centreline geometry.

aspirin, corticoids, vascular endothelial growth factor and brachytherapy, but none has achieved marked success [15]. Drug-eluting stents, stents coated with anti-proliferative agents, have attracted much attention. Improved patency is reported, when compared with bare-metal stents [16,17], but there are cost and safety implications, and the findings are still subject to analysis.

In recognition of the common non-planarity of arterial geometry and resulting three-dimensionality of intraluminal flow [18], we modified a commercially available bare-metal, nitinol, self-expanding stent by introducing a helical-centreline [19]. The modified stent having three-dimensional, helical-centreline geometry (figure 1) was deployed in one common carotid artery (CCA) of healthy pigs, with a straight-centreline, but otherwise identical, stent deployed in the contralateral CCA.

The work was conducted in two phases and is thus presented. The first phase [19] describes the implantation and follow-up procedures, the changes in arterial geometry and flow with both types of stent, and the lesser occurrence of IH in CCAs implanted with helical-centreline stents, when compared with straight-centreline stents. The second phase [20] further considers underlying mechanisms, among them that stenting can influence arterial Ad-MV and intraluminal blood vessel wall mass transport, including of oxygen.

2. Phase one

2.1. Methods

The animal studies were undertaken at Saint Joseph's Translational Research Institute (SJTRI), Atlanta, GA, USA. They involved 10 healthy female farm pigs (42.4 ± 0.97 kg, s.e.m.), given free access to clean water and fed a commercial pelleted chow diet, adequate to permit reasonable weight gain in growing animals.

2.1.1. Surgical and related procedures

Aspirin (81 mg) and plavix (75 mg) were administered daily from 3 days prior to surgery up to termination and flunixin 1–2 mg kg^{-1} was administered intramuscularly for pre-operative analgesia. After sedation, an ear vein was cannulated for infusions, the animals were intubated and limb lead electrocardiography was used. Intravenous heparin was administered to maintain an activated clotting time of greater than 5 min. An 8F femoral access sheath was placed in the right femoral artery via surgical cut down. An 8F J tip-shaped guide catheter was used to position a 0.035″ Cougar XT hydro-track guidewire in the LCCA/RCCA. Baseline angiography was recorded in two planes approximately 90° apart, to determine arterial three-dimensional geometry.

B-mode ultrasound and angiography were used to measure vessels for stent diameter selection. At the mid-section of vessels to be stented, one longitudinal and two transverse measurements were made and averaged to determine vessel diameter. All vessels were less than 5.3 mm in diameter and were implanted with a 6×80 mm self-expanding nitinol bare-metal stent. At implantation, the guide catheter was replaced by a 7F straight guide catheter, and the stent delivery system was positioned in the carotid artery. The stent (helical-centreline or straight-centreline) was deployed by slowly drawing back the retaining sheath. There was no use of ballooning. The contralateral CCA was then similarly implanted, but with the alternate type stent. The helical-centreline and straight-centreline stents were deployed randomly in the left or right CCA: five right and five left. Digital subtraction angiography (DSA), using contrast, was performed immediately after stent deployment to assess vessel geometry. In addition, small (neither volume nor flow-rate controlled) boluses of contrast were injected intraluminally to assess whether there was swirling and cross-mixing [21]. Doppler ultrasound was also used to detect swirling flow, using a technique described by How *et al*. [22].

Twenty-eight to 30 days after stent implantation, the animals were prepared, anaesthetized, and vessel access was achieved. Doppler ultrasound was used, as previously, to detect swirling flow. DSA was also repeated using contrast to determine vessel geometry, with small quantities of contrast injected as boluses to detect swirling. The animals were terminated by intravenous injection of potassium chloride while under surgical anaesthesia with inhalant isoflurane, and segments of CCA were harvested and processed histologically.

2.1.2. Histomorphometry and histopathology

Vessels were perfusion-fixed with 1.25% glutaraldehyde–5% formalin at approximately 100 mmHg pressure for a minimum of 10 min, either *in situ* or after careful excision.

They were then held in 10% neutral buffered formalin until further processing. They were dehydrated in a series of graded ethanol solutions to 100% and embedded in methyl methacrylate. Sections were cut, using a precision saw-and-grinding technique at the proximal, middle and distal segments of the stented vessels, and stained with paragon–toluidine blue and basic fuchsin. Embedding in polymeric resins renders cell-specific staining difficult and was not performed.

Histomorphometry: this was performed by individuals unaware of treatment group assignment. Each section was imaged by charge-coupled device camera. Morphometric analysis was performed by computerized planimetry on each of the sections. Luminal, intimal (luminal surface to internal elastic lamina) and medial (internal elastic lamina to external elastic lamina) cross-sectional areas were measured. To determine statistical significance, *p*-values were calculated using paired Student's *t*-tests with significance (*) indicated where $p < 0.05$.

Histopathology: sections were assessed for vessel wall response to stent implantation, including extent of injury, neointima formation, haemorrhage, necrosis, inflammation and calcification. Evaluation was performed using one or more low or high magnification images of each section. All histopathological parameters were evaluated on a semi-quantitative rating scale of: 0, none; 1, mild; 2, moderate; and 3, severe, where 0 represented the least response and 3 represented the greatest response of all tissues analysed in this study within each category. Endothelialization was

evaluated on a different grading scale, where 0 = 0–25% circumference coverage; 1 = 25–50% coverage; 2 = 50–75% coverage; 3 = 75–100% coverage.

2.2. Results

At implantation, there was no significant difference between the oversizing of the stents in the two groups. The helical-centreline stents were oversized by 23.3% ± 8.5 and the straight-centreline stents by 24.8% ± 10.4 ($p > 0.05$).

DSA with contrast, performed immediately following stent deployment, revealed helical deformation of helical-centreline stented but not straight-centreline stented CCAs (figure 2*a*). Images (including sequential still frames at 30 Hz) and attached video clips (figure 2*b*) show swirling of flow following bolus injections of contrast in a helical-centreline stented CCA and essentially axial passage of contrast in the contralateral, straight-centreline stented vessel. They appear to show, moreover, cross-mixing in the helical-centreline stented vessel, but not in the straight-centreline stented vessel. This is indicated by faster travel of the leading edge of contrast in the straight-centreline stented than helical-centreline stented vessel and faster travel of the tail of the contrast in the helical-centreline stented than straight-centreline stented vessel [21]. The amplitude of the helical-centreline stents was maintained from the time of implantation to the time of termination at 30 days.

Inspection of the transverse sections showed variation of intimal and medial thickness both circumferentially in sections from the same segment and between sections from proximal, middle and distal segments (figure 3).

Planimetric measurements averaged over the three (proximal, middle and distal) segments for the 10 animals showed intimal cross-sectional area (mm^2) to be significantly less in the helical-centreline stented than straight-centreline stented arteries, whereas medial cross-sectional area was not significantly different between the two groups (table 1). Luminal cross-sectional area was significantly larger in helical-centreline stented than straight-centreline stented vessels.

Cell-specific staining was, as noted, not undertaken. However, histological observations (figure 4) showed an intima consisting apparently of SMCs in an organized extracellular matrix, with uniform endothelial cell coverage and no difference between the straight-centreline stented and helical-centreline stented groups, with respect to mural thrombosis, or re-endothelialization scorings. Deep to the apparent smooth muscle layer (and notably near stent struts), cells were present with a generally circular morphology and containing vesicles, suggesting that they were inflammatory cells, most probably macrophages. These cells were more numerous in the sections from the straight-centreline stented than helical-centreline stented vessels, but this apparent difference may have been due to the larger intima in the former vessels.

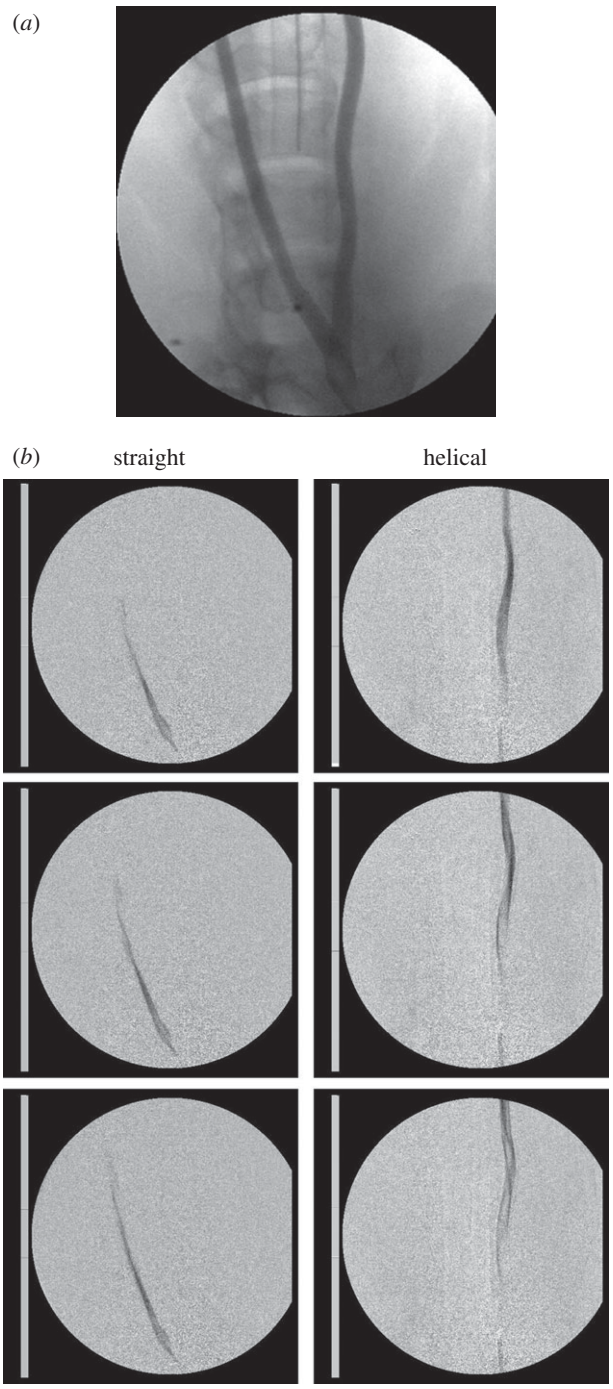

Figure 2. (*a*) PA (posterior–anterior) angiogram (supplemented by lateral angiograms, not shown) shows helical deformation of the animal's left (helical-centreline stented) CCA but not of the right (straight-centreline stented) CCA. (*b*) PA angiograms and video clips (see electronic supplementary material) after bolus injection of contrast. Interframe interval 0.033 s, frame sequence is from above downward, contrast injection is at bottom of frame. Swirling is seen in helical-centreline stented CCA but not in the straight-centreline stented contralateral CCA. Consistent with helicity-induced cross-mixing, leading edge of contrast appears to travel faster in straight-centreline stented than helical-centreline stented vessel, whereas tail of contrast appears to travel faster in helical-centreline stented than in straight-centreline stented vessel [21]. The video clip is available online only (see electronic supplementary material). To facilitate viewing, the video clip has been slowed to one-third *in vivo* speed.

3. Phase two

3.1. Methods

3.1.1. Histomorphometry

3.1.1.1. Intima–media ratio

Transverse sections from the proximal, middle and distal segments of both the helical-centreline stented and straight-centreline stented CCAs were re-examined. Using ProgResCapturePro v. 2.5 software, the cross-sectional area of the adventitia was measured together with the thickness of the intima and of the media at three or four locations

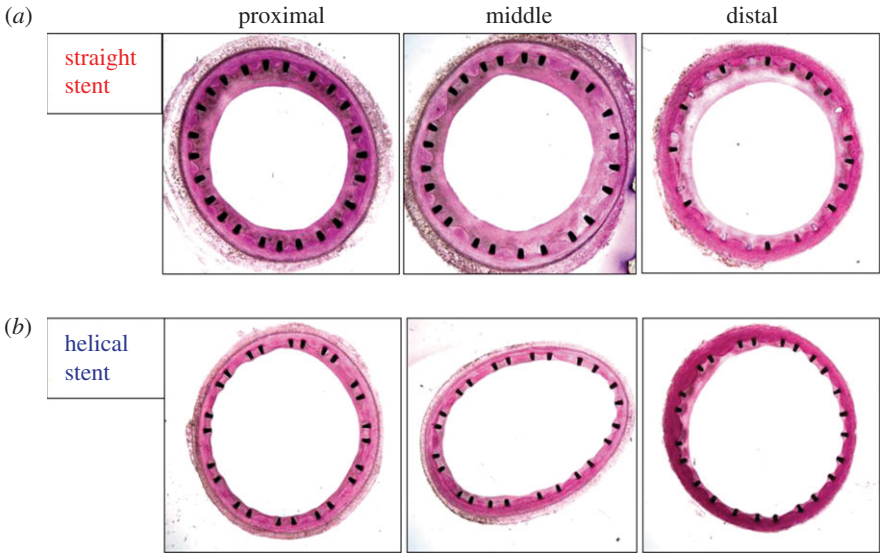

Figure 3. Transverse sections of proximal, middle and distal segments of CCAs, one month after stent deployment. (*a*) Straight-centreline stented. (*b*) Helical-centreline stented.

Table 1. Average (±s.d.) intimal and medial area for the three (proximal, middle and distal) segments for the 10 helical-centreline stented and 10 straight-centreline stented vessels.

group		intimal area (mm^2)	medial area (mm^2)	luminal area (mm^2)
straight-centreline stent ($n = 10$)	mean	6.70	5.12	14.25
	s.d.	1.13	0.43	0.81
helical-centreline stent ($n = 10$)	mean	4.59	4.96	17.38
	s.d.	1.30	0.62	1.48
	p (*t*-test)	0.001	0.38	<0.001

around the circumference of the vessel section to obtain a representative value of the intima-to-media ratio (IMR).

3.1.1.2. Adventitial microvessel number

Using ImageJ software, the number of Ad-MV was determined for each animal, for both the helical-centreline stented and straight-centreline stented CCAs. Vessels with circular or elliptical cross sections, or lying parallel to the section surface were counted (see electronic supplementary material, image available online only). On average, three sections were studied from each of the proximal, middle and distal segments. Measurements were performed by a single expert observer blinded to the stent type used. Blinded measurements were repeated by the same observer after a six month interval, and the two sets of measurements were compared. The two sets of measurements were found to be consistent and averaged.

3.2. Results

Inspection of the transverse arterial sections (figure 3) showed compression of the media in both the helical-centreline (three-dimensional) stented and straight-centreline stented vessels, as revealed by its herniation between the stent struts. It was thought that the minimal thickness of the media circumferentially would give an indication as to whether helical-centreline stenting caused more or less wall deformation than straight-centreline stenting. However, measurements made at the middle segment with on-screen callipers showed no significant difference in minimal medial thickness ($p = 0.24$) between the two stent types.

As shown in figure 5, IMR was significantly higher overall in the straight-centreline stented (1.10 ± 0.11) than helical-centreline stented vessels (0.69 ± 0.11; $p < 0.01$). In addition, IMR was significantly lower in the distal (0.32 ± 0.05) than proximal (1.02 ± 0.28), or middle (0.99 ± 0.15) segments in the helical-centreline stented vessels ($p < 0.01$) and also significantly lower than in the proximal (1.34 ± 0.11), middle (1.25 ± 0.09) or distal (1.09 ± 0.13) segments in the straight-centreline stented vessels ($p < 0.01$).

Average intimal thicknesses (±s.d.) for the helical-centreline and straight-centreline stented groups were respectively 0.2 ± 0.09 and 0.37 ± 0.08 ($p < 0.05$), that is intimal thickness was on average 45% less in the helical-centreline stented vessels. Variation in intimal thickness between the different arterial segments is considered below.

No correlation was observed between adventitial microvessel number and section thickness. The results are therefore presented as adventitial microvessel density (number of microvessels per unit adventitial area). No correction was made for adventitial area, because this was not significantly different between the helical-centreline stented and straight-centreline stented vessels. Averaging the results for the proximal, middle and distal segments, for the two groups, adventitial microvessel density was significantly lower in the helical-centreline stented than straight-centreline stented arteries, the values being: helical-centreline stented 130.8 ± 7.2; straight-centreline stented 216.3 ± 19.1 ($p < 0.0006$,***). The difference between

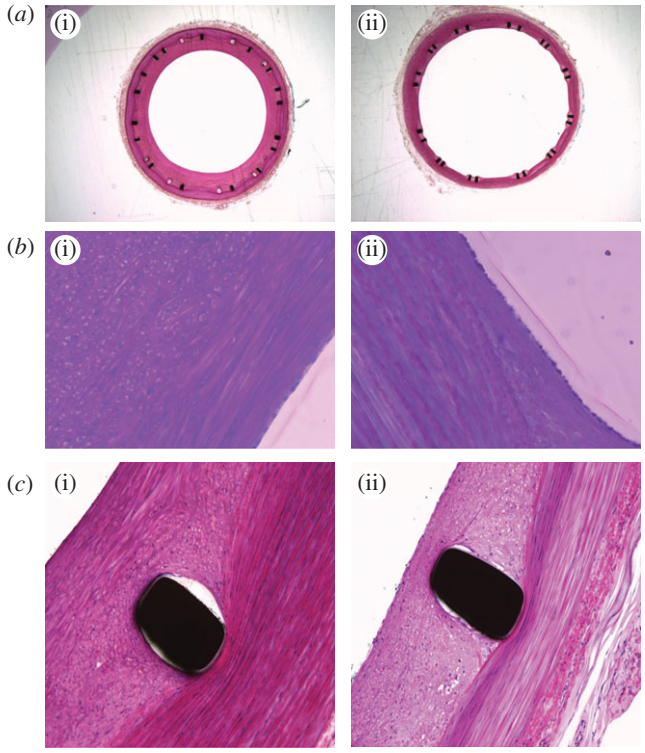

Figure 4. (*a*) Low magnification fuchsin stained cross sections of porcine common carotid arteries with (i) straight-centreline stent implanted and (ii) helical-centreline stent implanted. (*b*) Same cross sections as in figure 4*a* (40× magnification). An endothelial cell layer is visible in both (i) and (ii), respectively, straight-centreline and helical-centreline stented. At the luminal edge elongated cells resembling smooth muscle cells are visible. Deep to this layer (i), cells are present with a more circular conformation and intracellular vesicles, suggesting they are inflammatory, probably macrophages. (*c*) Same arterial cross-sections as in figures 4*a*, 4*b* (40× magnification) but in proximity to stent struts.

helical-centreline stented and straight-centreline stented vessels was pronounced in the proximal and middle segments, but not significant in the distal segments (figure 6).

4. Discussion

We implanted a helical-centreline, bare-metal, nitinol, self-expanding stent in one CCA of 10 healthy pigs and a straight-centreline, but otherwise identical, stent in the contralateral CCA. Both types of stent deformed the vessels. However, the former also deformed them helically and generated swirling (and seemingly cross-mixing) of the intraluminal flow. Geometrical and flow changes persisted up to the time of sacrifice at four weeks. Histology revealed the intimal cross-sectional area to be significantly less, overall, in the helical-centreline stented than straight-centreline stented arteries. By contrast, the medial cross-sectional area was not significantly different between the two groups of arteries, whereas luminal cross-sectional area was significantly greater in helical-centreline stented than straight-centreline stented vessels. IMR was significantly lower in those vessels in which a helical-centreline stent was present. Moreover, there appeared to be significantly fewer Ad-MV in helical-centreline stented compared with straight-centreline stented arteries.

We consider these findings and possible underlying mechanisms. Numerical studies of steady flow in a helical tube with geometry and flow similar to those in the present porcine study [19] show WSS to be higher on average than with corresponding Poiseuille flow (figure 7). As shown by ultrasound, the flow in this study was pulsatile. The combination of flow pulsatility and conduit centreline helicity will result in a sweeping motion of the Dean vortices, which would reduce extremes (both maxima and minima) of WSS. Nevertheless, it can be expected that with pulsatility of the same mass flux in the same geometry, WSS will be higher, on average, than with Poiseuille flow [23,24].

The numerical studies also show that flow in a relevant helical conduit causes intraluminal swirling and cross-mixing, which develops with distance and persists for a short distance in a straight conduit downstream of the helical conduit (figure 8).

Supportive of the proposal that elevation of WSS suppresses IH, Carlier *et al*. [10] enhanced local WSS by placing a flow divider at the centreline of stents implanted in the external iliac arteries of rabbits and found significantly less neointimal hyperplasia (analogous to IH) in vessels with the flow divider than without it. Shinke *et al*. [19] proposed elevation of WSS, resulting from intraluminal swirling, as responsible for the lesser occurrence of IH in the helical-centreline stented than straight-centreline stented CCAs. That proposition would seem acceptable. However, consideration should also be given to possible involvement of blood–wall mass transport, including of oxygen, arguments for which are now examined.

Stenting of arteries has been shown to render them locally hypoxic [1,2] and the intimal cross-sectional area in the stented regions in arteries was found highly correlated with adventitial microvessel number. Ad-MV number can be considered representative of tissue hypoxia, because it increases after stenting [2] and hypoxia is a major stimulus for angiogenesis [25]. Intraluminal swirling in a helical conduit can not only enhance WSS, but also mass transport of fluid phase-controlled molecular species, including oxygen [26,27], between intraluminal blood and the vessel wall. Thus, intraluminal swirling can enhance intraluminal blood–vessel wall oxygen transport both by increasing wall shear (WS) rate and, by convection, by virtue of intraluminal mixing [23,27].

Motivated by these observations and that arterial wall mass transport depends on both the vasa vasorum and intraluminal flow, we attempted to quantify the Ad-MV in the helical-centreline stented and straight-centreline stented arteries. We found Ad-MV density to be significantly lower in the former than latter vessels. However, quantification of Ad-MV is challenging, implying the need for caution in interpreting these results. Refined methods of quantifying Ad-MV and direct approaches to assessing wall hypoxia are therefore indicated [1,2].

Stenting evidently deforms the arterial wall. We are unaware of studies of the immediate effects of arterial stenting on Ad-MV morphology, but distension of arteries by increasing their transmural pressure caused Ad-MV cross-sections to change from circular to elliptical, their hydraulic resistance to rise, and their flow to fall, potentially impairing wall perfusion [28]. Unlike elevation of arterial transmural pressure, stenting will not increase Ad-MV intraluminal pressure. It could, therefore, affect Ad-MV morphology and flow more severely than transmural pressure elevation.

Relevant to these observations, microelectrode measurements made in the aortas of rabbits immediately following stent deployment showed thinning of the vessel wall and decrease of oxygen tension throughout the wall, with values returning towards control at 28 days [1]. These studies

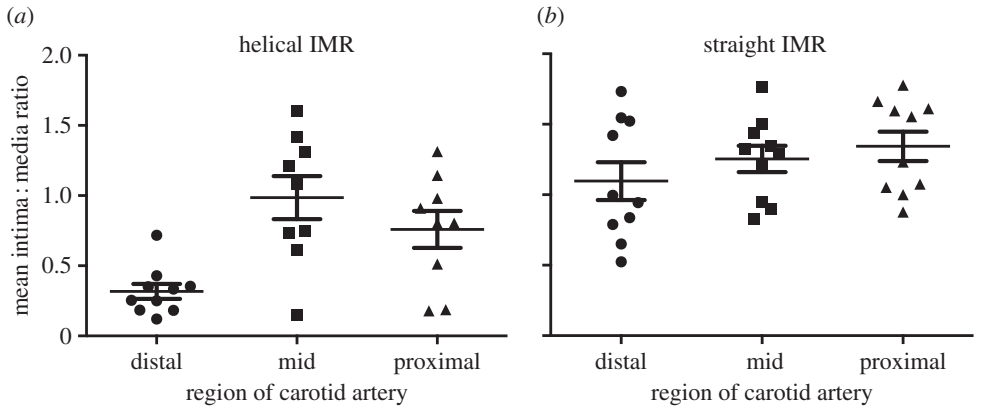

Figure 5. (*a*–*b*) IMRs in the helical-centreline stented and straight-centreline stented CCAs.

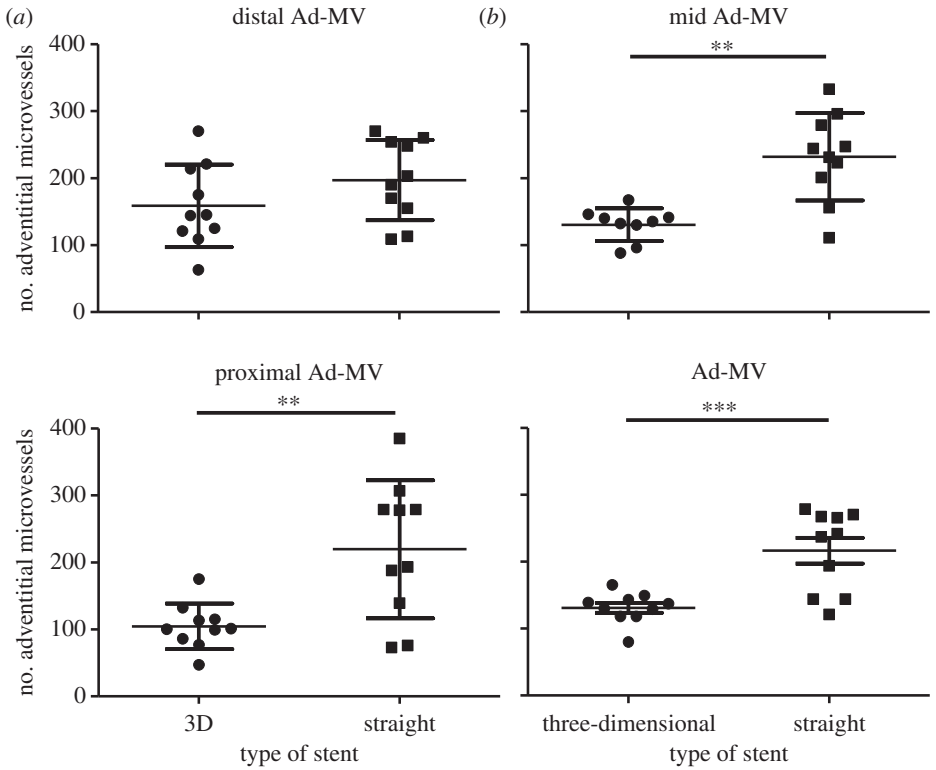

Figure 6. Number of adventitial microvessels in proximal, middle and distal segments of the helical-centreline stented and straight-centreline stented CCAs.

also showed deployment of oversized stents to further lower artery wall oxygen tension. Additionally relevant, immunohistochemical studies by Cheema *et al*. [2] showed hypoxia to persist in coronary arteries in pigs at one and four weeks after stent implantation and localization of the hypoxia to the medial/adventitial border.

We now consider the findings in the different (proximal, middle and distal) segments of the straight-centreline and helical-centreline stented arteries. The flow in these vessels can be expected to develop with distance. In the straight-centreline case, presuming the vessel to be straight, circular, uniform in cross section and unbranched, WSS will fall with distance. In the helical-centreline case, the flow will additionally depend on the pitch and amplitude ratio (amplitude/diameter) of the helical vessel. Assuming diameter and other geometrical parameters to remain constant along the vessel, WSS will, in contrast with the straight-centreline case, rise with distance. If WSS lessens IH, then the lower IMR in the distal than proximal and middle segments of the helical-centreline stented vessels could relate to a rise of WSS, associated with flow development.

Measurements made at the time of stent implantation from computed tomography data show, however, that in both the helical-centreline stented and straight-centreline stented CCAs there is tapering of the lumen in the downstream direction, with cross-sectional area decreasing on average from 24 to 20 mm^2 between the proximal and distal segments. Provided mass flux remained essentially constant along the vessels, such tapering would increase WSS proceeding in the downstream direction and could contribute to explaining the lower IMR in distal than proximal and middle segments of helical-centreline stented CCAs. It could, moreover, help explain the tendency for IMR to be lower—rather than higher—as predicted by boundary layer growth, proceeding from proximal to distal segments of straight-centreline stented vessels (figure 5).

We also consider wall mass transport in the different arterial segments. Given that swirling is predicted to enhance intraluminal blood–wall oxygen transport and that hypoxia

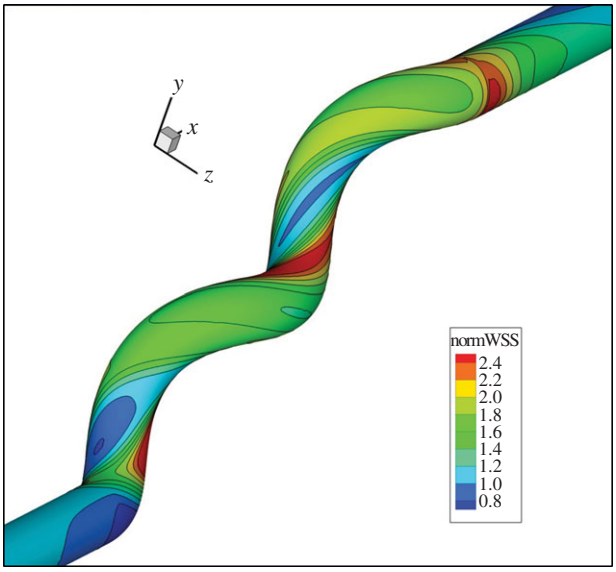

Figure 7. CFD study illustrating the distribution of wall shear stress in a helical conduit under steady flow conditions, normalized by Poiseuille flow. Reynolds number 200, amplitude ratio 0.5, pitch 5 diameters, parameters similar to those obtained in the CCAs of the helical-centreline stented pigs [19] (P. Franke 2004, unpublished data).

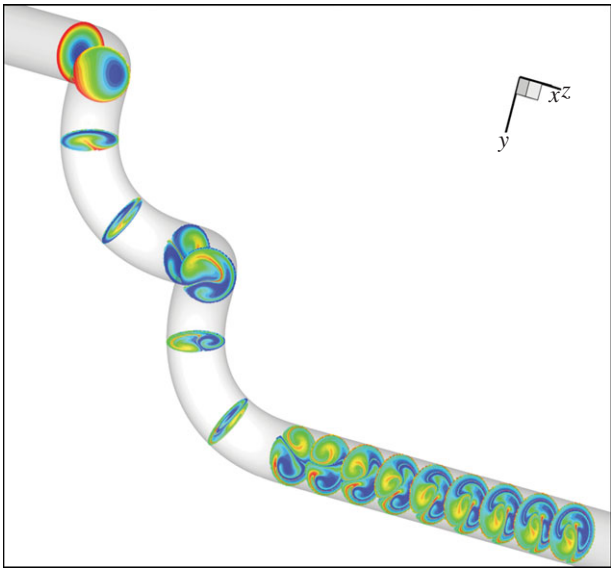

Figure 8. CFD seeded disc study, illustrating swirling and mixing in a helical conduit and its persistence for a short distance in a straight conduit downstream of the helical conduit. Reynolds number 200, amplitude ratio 0.5, pitch 5 diameters, parameters similar to those obtained in the CCAs of the helical-centreline stented pigs [19]. Unlike *in vivo*, model flow is steady. (P. Franke 2004, unpublished data).

is a major stimulus for angiogenesis [2,25], Ad-MV values should be lower in the distal than proximal and middle segments of helically stented vessels. Why that expectation is not fulfilled is unclear. Additional investigation is warranted concerning characterization of the flow field in arteries. Given that intraluminal wall shear appears to protect against IH, a complementary explanation for the lesser occurrence of IH at helical-centreline stented than straight-centreline stented vessels could be that straight-centreline stenting suppresses the physiological three-dimensionality of vessels.

The study reports significantly less IH in the common carotid arteries of healthy pigs implanted one month earlier with helical-centreline stents compared with vessels implanted contralaterally with straight-centreline stents. Medial cross-sectional area was not different between the two types of stent, but luminal cross-sectional area was significantly larger in helical-centreline stented than straight-centreline stented vessels, a finding potentially of considerable haemodynamic and pathological importance.

The findings imply the involvement of both WSS and blood–wall oxygen transport. It would, therefore, be of interest to distinguish their individual contributions. However, this is not a simple task. Because the diffusion coefficient for momentum significantly exceeds that for mass, the possibility exists of distinguishing their contributions in the absence of mixing, say in a straight pipe downstream of a bend. By contrast, their contributions will tend to co-locate where there is mixing [23,24]. Supportive of the hypothesis that helical-centreline stented CCAs were less hypoxic than straight-centreline stented vessels is that supplementary oxygen reduced the severity of IH after arterial stenting in animals [29].

The porcine studies were performed at SJTRI Atlanta, GA, USA. They were performed in accordance with the requirements of the Animal Welfare Act and amendments. Compliance was accomplished by conforming to the standards in the Guide for the Care and the Use of Laboratory Animals, Institute of Laboratory Animal Research, National Academy Press, latest edition. Prior to study execution, experimental procedures were reviewed by SJTRI licensed veterinarians and approved by SJTRI Institutional Animal Care and Use Committee.

Acknowledgements. Figures 1 and 2*a*,*b* (including video clips—available online only), 3, 4*a*, 4*c* and image of segment of artery stained with basic fuchsin and showing microvessels (supplementary material—available online only) are reproduced with permission—Copyright Veryan Medical Ltd. Figures 7 and 8 are reproduced with permission—Peter Franke. The support is acknowledged of the Henry Smith Charity, the Garfield Weston Foundation and GE Healthcare. C.G.C. is a consultant to Veryan Medical Limited.

References

1. Santilli SM, Tretinyak AS, Lee ES. 2000 Transarterial wall oxygen gradients at the deployment site of an intra-arterial stent in the rabbit. *Am. J. Physiol. Heart Circ. Physiol.* **279**, H1518–H1525.
2. Cheema AN *et al.* 2006 Adventitial microvessel formation after coronary stenting and the effects of SU11218, a tyrosine kinase inhibitor. *J. Am. Coll. Cardiol* **4.7**, 1067–1075. (doi:10.1016/j.jacc.2005.08.076)
3. Nikol S, Huehns TY, Weir L, Wight TN, Hofling B. 1998 Restenosis in human vein bypass grafts. *Atherosclerosis* **139**, 31–39. (doi:10.1016/S0021-9150(98)00050-1)
4. Rotmans JI, Velema E, Verhagen HJM, Blankensteijn JD, Kastelein JJP, de Kleijn DPV, Yo M, Pasterkamp G, Stroes ESG. 2003 Rapid, arteriovenousgraft failure due to intimal hyperplasia: a porcine, bilateral, carotid arteriovenous graft model. *J. Surg. Res.* **113**, 161–171. (doi:10.1016/S0022-4804(03)00228-2)
5. Dember M, Dixon BS. 2007 Early fistula failure: back to basics. *Am. J. Kidney Dis.* **50**, 696–699. (doi:10.1053/j.ajkd.2007.09.006)
6. Lemson MS, Daemen MJAP, Kitslaar PJEH, Tordoir JHM. 1999 A new animal model to study intimal

hyperplasia in arteriovenousfistulas. *J. Surg. Res.* **85**, 51–58. (doi:10.1006/jsre.1999.5566)

7. Lee T, Roy-Chaudhury R. 2009 Advances and new frontiers in the pathophysiology of venous neointimal hyperplasia and dialysis access stenosis. *Adv. Chronic Kidney Dis.* **16**, 329–338. (doi:10.1053/j.ackd.2009.06.009)
8. Wang Y, Krishnamoorthy M, Banerjee R, Zhang JH, Rudich S, Holland C, Arend L, Roy-Chaudhury P. 2008 Venous stenosis in a pig arteriovenous fistula model—anatomy, mechanisms and cellular phenotypes. *Nephrol. Dial. Transplant.* **23**, 525–533. (doi:10.1093/ndt/gfm547)
9. Guzman LA, Mick MJ, Arnold AM, Forudi F, Whitlow PL. 1996 Role of intimal hyperplasia and arterial remodeling after balloon angioplasty. *ATVB* **16**, 479–487. (doi:10.1161/01.ATV.16.3.479)
10. Carlier SG *et al*. 2003 Augmentation of wall shear stress inhibits neointimal hyperplasia after stent implantation: inhibition through reduction of inflammation? *Circulation* **107**, 2741–2746. (doi:10.1161/01.CIR.0000066914.95878.6D)
11. Chiu JJ, Chien S. 2011 Effects of disturbed flow on vascular endothelium: pathophysiological basis and clinical perspectives. *Physiol. Rev.* **91**, 327–387. (doi:10.1152/physrev.00047.2009)
12. Rogers C, Tseng DY, Squire JC, Edelman ER. 1999 Balloon–artery interactions during stent placement: a finite element analysis approach to pressure, compliance, and stent design as contributors to vascular injury. *Circ. Res.* **84**, 378–383. (doi:10.1161/01.RES.84.4.378)
13. Timmins LH, Miller MW, Clubb Jr FJ, Moore Jr JE. 2011 Increased artery wall stress post-stenting leads to greater intimal thickening. *Lab Invest.* **91**, 955–967. (doi:10.1038/labinvest.2011.57)
14. Virmani R, Farb A. 1999 Pathology of in-stent restenosis. *Curr. Opin. Lipidol.* **10**, 499–506.
15. Mauro MA. 2004 The battle of intimal hyperplasia in the war against femoropopliteal disease. *Radiology* **231**, 299–301. (doi:10.1148/radiol.2312032127)
16. Dake MD, Van Alstine WG, Zhou Q, Ragheb AO. 2011 Polymer-free paclitaxel-coated Zilver PTX stents: evaluation of pharmacokinetics and comparative safety in porcine arteries. *J. Vasc. Interv. Radiol.* **22**, 603–610. (doi:10.1016/j.jvir.2010.12.027)
17. Morice MC *et al*. for the RAVEL Study Group. 2002 A randomized comparison of a sirolimus-eluting stent with a standard stent for coronary revascularization. *New Engl. J. Med.* **346**, 1773–1780. (doi:10.1056/NEJMoa012843)
18. Caro CG, Doorly DJ, Tarnawski M, Scott KT, Long Q, Dumoulin CL. 1996 Non-planar curvature and branching of arteries and non-planar-type flow. *Proc. R. Soc. Lond. A* **452**, 185–197. (doi:10.1098/rspa.1996.0011)
19. Shinke T *et al*. 2008 Novel helical stent design elicits swirling blood flow pattern and inhibits neointima formation in porcine carotid arteries. *Circulation* **118**, S1054.
20. Caro CG, Seneviratne A, Monaco C, Hou D, Singh J, Burke M, Heraty K, Krams R, Coppola G. 2011 Arterial stent intimal hyperplasia: role of hypoxia and blood–wall oxygen transport, physiology 2011, Oxford. *Proc. Physiol. Soc.* **23**, C79.
21. Caro CG. 1966 The dispersion of indicator flowing through simplified models of the circulation and its relevance to velocity profile in blood vessels. *J. Physiol.* **185**, 501–519.
22. How TV, Fisher RK, Brennan JA, Harris PL. 2006 Swirling flow pattern in a non-planar model of an interposition vein cuff anastomosis. *Med. Eng. Phys.* **28**, 27–35. (doi:10.1016/j.medengphy.2005.04.016)
23. Coppola G, Caro CG. 2008 Oxygen mass transfer in a model three-dimensional artery. *J. R. Soc. Interface* **5**, 1067–1075. (doi:10.1098/rsif.2007.1338)
24. Coppola G, Caro CG. 2009 Arterial geometry, flow pattern, wall shear and mass transport: potential physiological significance. *J. R. Soc. Interface* **6**, 519–528. (doi:10.1098/rsif.2008.0417)
25. Shweiki D, Itin A, Soffer D, Keshet E. 1992 Vascular endothelial growth factor induced by hypoxia may mediate hypoxia-initiated angiogenesis. *Nature* **359**, 843–845. (doi:10.1038/359843a0)
26. Tarbell JM. 2003 Mass transport in arteries and the localization of atherosclerosis. *Annu. Rev. Biomed. Eng.* **5**, 79–118. (doi:10.1146/annurev.bioeng.5.040202.121529)
27. Litster S, Pharoah JG, Djilali N. 2005 Convective mass transfer in helical pipes: effect of curvature and torsion. *Heat Mass Transf.* **42**, 387–397. (doi:10.1007/s00231-005-0029-y)
28. Maurice G, Wang X, Lehalle B, Stoltz JF. 1998 Modeling of elastic deformation and vascular resistance of arterial and venous vasa vasorum. *J. Malad. Vasc.* **23**, 282–288.
29. Tretinyak AS, Lee ES, Uema K, d'Audiffret AC, Caldwell MP, Santilli SM. 2002 Supplemental oxygen reduces hyperplasia after intra-arterial stenting in the rabbit. *J. Vasc. Surg.* **35**, 982–987. (doi:10.1067/mva.2002.123090)